Tuning the Electronic and Optical Properties of Graphene Quantum Dots via Cu Dimer Doping: A DFT Study

Hawraa Jaber Naser, Maryam Salman Sarbod, Fouad Nimr Ajeel*

Department of Physics, College of Science, University of Sumer, Rifai 64005, Iraq

***Corresponding Author**

DOI: https://dx.doi.org/10.51584/IJRIAS.2025.10120034

Received: 24 December 2025; Accepted: 30 December 2025; Published: 06 January 2026

ABSTRACT

Graphene quantum dots (GQDs) are emerging as promising nanomaterials for next-generation energy devices due to their tunable electronic and optical properties. However, optimizing their band gap and charge transport remains a challenge. In this study, we employ density functional theory (DFT) to investigate the influence of Cu dimer doping on the structural, electronic, and optical characteristics of GQDs. Our results show that Cu_2 doping reduces the band gap significantly from 4.130 eV in pristine GQDs to as low as 1.059 eV enabling enhanced electrical conductivity and extended optical absorption into the infrared region. The Cu_2-2 configuration demonstrates the most favorable electronic delocalization and dipole behavior, highlighting its suitability for optoelectronic and energy-related applications. These modifications improve the material's potential for use in solar energy harvesting, infrared photodetectors, and energy storage devices. This study demonstrates a viable pathway to engineer low-band-gap, highly conductive GQDs for wearable electronics.

Keywords: Graphene Quantum Dots, Cu Dimer, DFT, Band Gap Engineering, Electronic Properties.

INTRODUCTION

In recent years, the pursuit of sustainable energy solutions has accelerated interest in nanomaterials capable of offering superior efficiency, stability, and adaptability across energy storage and conversion technologies [1-3]. Among these, graphene quantum dots (GQDs) have emerged as a prominent class of carbon-based nanomaterials with unique physical and chemical features such as quantum confinement, large surface-to-volume ratio, and edge effects [4-7]. These properties render them promising candidates for energy-related applications, including supercapacitors, solar cells, and batteries [4]. Compared to bulk graphene, GQDs offer enhanced band gap tunability, better dispersion, and chemical reactivity, which are essential in energy harvesting technologies [8, 9].

The ability to modify the intrinsic properties of GQDs via doping has created a pathway toward customizing their performance for specific applications [10-12]. Doping GQDs with heteroatoms like boron, nitrogen, or metals has been shown to introduce mid-gap states, modify electron distribution, and improve optical absorption in broader spectra [13, 14]. For instance, boron doping enhances the p-type conductivity and ion adsorption capacity, which is critical in high-performance supercapacitors [15, 16]. Similarly, sulfur and nitrogen functionalization can reduce recombination of charge carriers, enhancing photocatalytic activity for hydrogen evolution and pollutant degradation [17, 18]. These advancements in doping strategies have significantly expanded the practical utility of GQDs across a variety of clean energy platforms [19].

Moreover, the integration of doped GQDs into composite nanomaterials has led to remarkable performance enhancements in energy devices. Hybrid systems composed of GQDs and carbon nanotubes, conducting polymers, or metal oxides benefit from synergistic effects that improve electron transport and mechanical stability [20]. For example, GQD-based electrodes have achieved high specific capacitances and cycle stability in electric double-layer capacitors due to their abundant edge sites and pseudocapacitive behavior [4, 21]. In optoelectronics, quantum dot nanocomposites facilitate better charge separation and light absorption in the visible and near-infrared range, making them suitable for solar harvesting and photoelectrochemical cells [22]. Despite significant achievements, challenges remain in controlling size distribution, optimizing dopant placement, and ensuring long-term stability of doped GQDs [23].

ISSN No. 2454-6194 | DOI: 10.51584/IJRIAS |Volume X Issue XII December 2025

In light of these developments, the present study employs density functional theory (DFT) to explore the impact of copper dimer (Cu_2) doping on the structural, electronic, and optical properties of graphene quantum dots. The focus is on examining how Cu_2 dopants alter band gap energy, charge density distribution, and absorption spectra, particularly in the visible to infrared range. Such tuning is critical for improving energy device performance, especially in solar energy conversion and energy storage systems where low band gap and high charge mobility are desirable [24]. The study identifies optimal Cu_2 configurations that exhibit favorable electronic delocalization and dipole characteristics, supporting their integration into next-generation nanomaterials for green energy technologies. Ultimately, this research aims to contribute to the rational design of low-band-gap, conductive GQD-based materials aligned with the goals of energy sustainability and device miniaturization.

Computational Methods

These computational evaluations are intended to guide the design of GQD-based nanomaterials tailored for energy harvesting and storage applications, where fine-tuning of electronic and optical characteristics directly impacts device performance. One of the components is the $C_{24}H_{12}$ graphene quantum dot, which is made up of seven benzene rings. The density functional theory using Gaussian package 09, B3LYP, and 6-31G performed the optimization procedure for the $C_{24}H_{12}$ structure [25-28]. GQDs have an energy gap (E_g), Fermi level (E_{FL}), highest occupied molecular orbital energies (E_{HOMO}), lowest unoccupied molecular orbital energies (E_{LUMO}), and electronic density of states (DOS) resolution. The density functional theory gives useful chemical reactivity parameters for studying reactivity patterns, excited states, and toxicity studies. The metrics comprised chemical hardness (η), chemical softness (S), chemical potential (μ), and electrophilicity index (ω) are presented as [29-31]:

$$\mu = -\frac{(IP + EA)}{2} \tag{1}$$

$$\eta = \frac{(IP - EA)}{2} \tag{2}$$

$$S = \frac{1}{\eta} \tag{3}$$

$$\omega = \frac{\mu^2}{2\eta} \tag{4}$$

Koopman's theorem may be applied to both the ionization potential (IP) and the electron affinity (EA), yielding the following formula. [32, 33]:

$$IP = -E_{\mathrm{HOMO}} \tag{5}$$

$$EA = -E_{\mathrm{LUMO}} \tag{6}$$

Furthermore, we use the following formula to compute both the electronic band gap and the energy of the Fermi level [25, 34]:

$$E_{\mathrm{g}} = E_{\mathrm{LUMO}} - E_{\mathrm{HOMO}} \tag{7}$$

$$E_{\mathrm{FL}} = \frac{(E_{\mathrm{HOMO}} + E_{\mathrm{LUMO}})}{2} \tag{8}$$

The formation energy (E_F) quantifies a system's thermodynamic stability in the presence of defects or doping. This figure represents the amount of energy required to introduce a defect or dopant into the material. The general formula for finding E_F is given below. [35, 36]:

$$E_{\mathrm{F}} = E_{\mathrm{doped}} - E_{\mathrm{pristine}} - \mu_{Cu} + \mu_{\mathrm{C}} \tag{9}$$

ISSN No. 2454-6194 | DOI: 10.51584/IJRIAS |Volume X Issue XII December 2025

where E_{doped} is the total energy of the GQD doped with a Cu atom, and E_{pristine} is the total energy of the undoped (pure) GQD. The term μ_{Cu} denotes the chemical potential of the copper atom, typically derived from bulk copper or a reference phase. μ_{C} represents the chemical potential of the carbon atom that is replaced during the doping process.

RESULTS AND DISCUSSIONS

Figure 1(a) depicts pristine graphene quantum dots with a 7-benzene ring and an average C-C bond length of 1.42 Å, similar with earlier reported results [25, 27, 28]. To gain a thorough knowledge of the changes in electronic characteristics of pure quantum dots, it is necessary to investigate the electronic density of states of GQDs before and after atoms of carbon substitution with Cu dimers.

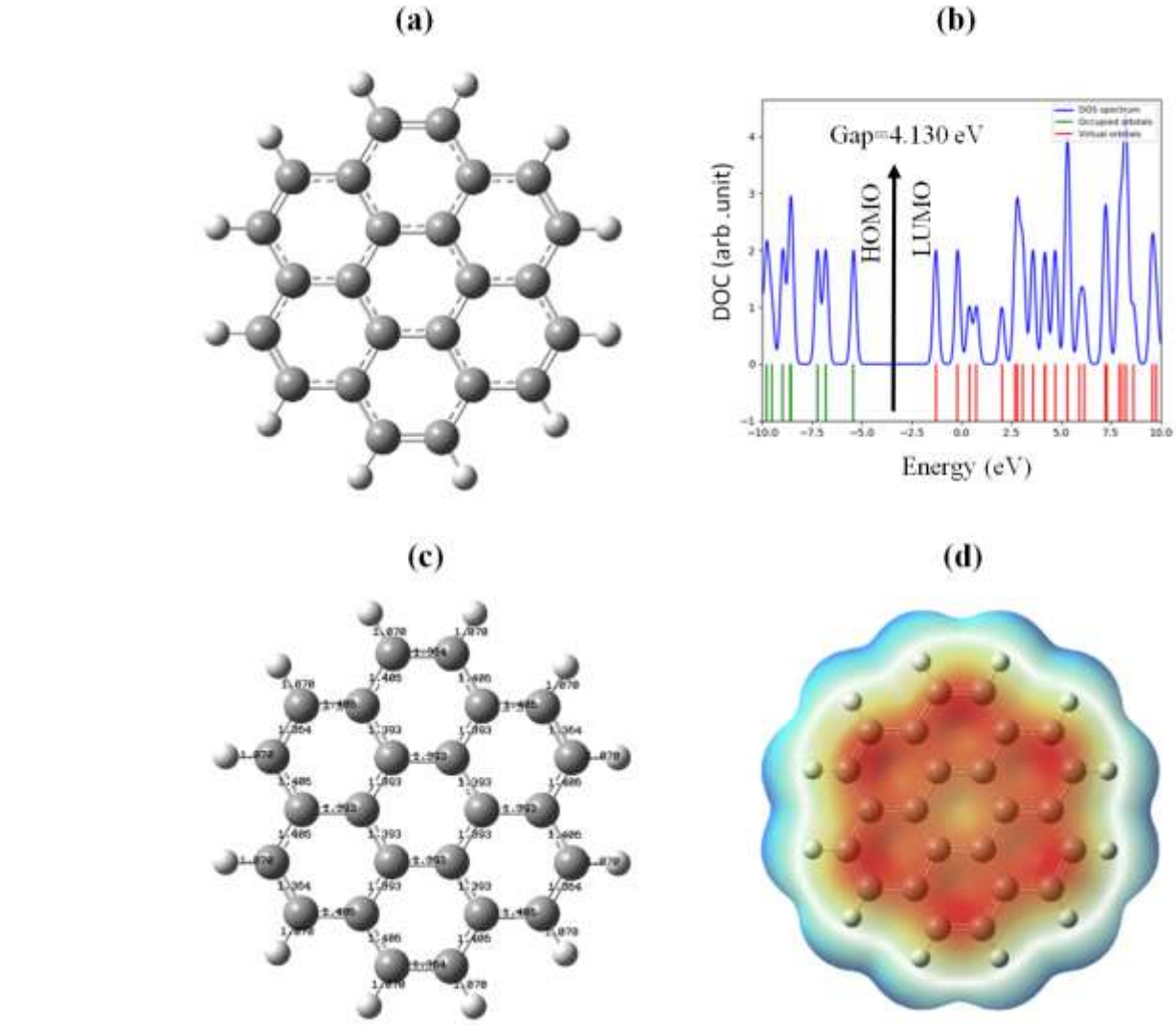

Figure 1: (**a**) Pristine graphene quantum dot structure, (**b**) density of state, (**c**) structured geometries and bond lengths, (**d**) molecule electrostatic potential graphic for the gas phase.

The pristine GQD structure is shown in Fig. 1(a), which has a hexagonal arrangement of carbon atoms with hydrogen atoms at the end. The density of states spectrum in Fig. 1(b) shows a substantial energy gap (4.130 eV) between the HOMO and LUMO orbitals, demonstrating the semiconducting nature of the dot. Figure 1(c) shows the bond lengths within the GQD structure, emphasizing the regularity of the sp^2-hybridized carbon network. The molecular electrostatic potential (MEP) map is then shown in Fig. 1(d), with red regions indicating electron-rich zones and blue regions indicating electron-deficient areas, representing the charge distribution inside the molecule.

Then, introducing Cu dimer at different sites affects the electronic properties of GQD. As shown in Fig. 2. Four types of Cu dimers are assumed: (a) Cu and Cu atoms are doped at ortho position (Cu_2-1), (b) Cu or Cu atoms are placed adjacent to one another in meta position (Cu_2-2), (c) Cu and Cu are at para position (Cu_2-3),

ISSN No. 2454-6194 | DOI: 10.51584/IJRIAS |Volume X Issue XII December 2025

and (d) Cu_2 pair is at ortho position but the distance between two Cu dimers is large (Cu_2-4). The electronic characteristics of quantum dots containing Cu dimers were examined. Figure 3 depicts the optimized structures of four distinct configurations: Cu_2-1, Cu_2-2, Cu_2-3, and Cu_2-4, as well as their related density of states spectra. The band gaps for each configuration were calculated using the energy difference between the HOMO and LUMO orbitals. The pure GQD has a rather high band gap, which is considerably affected by the addition of Cu dimers.

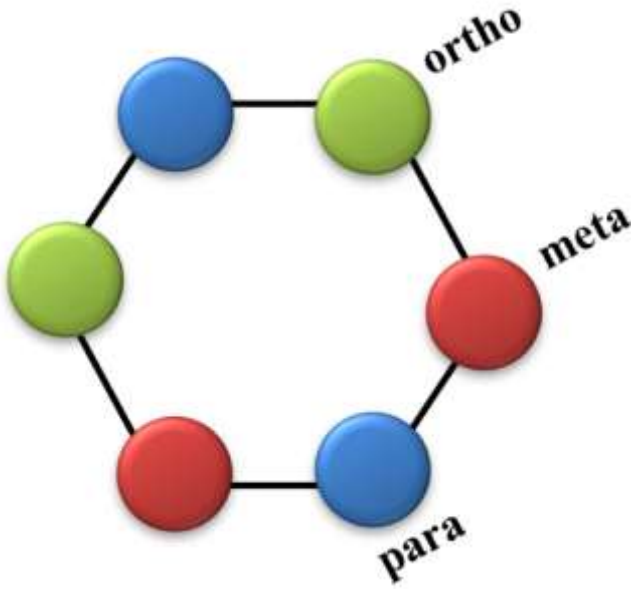

Figure 2: A diagrammatic representation showing the ortho, the meta, and the para places of doping inside the honeycomb structure

As seen in Fig. 3(a), the Cu_2-1 structure has a band gap of 1.939 eV, which is a significant decrease compared to the pristine dot, implying that the localized Cu_2 interactions marginally disrupt the electronic states. Moving on to Fig. 3(b), the Cu_2-2 structure has a substantially lower band gap of 1.059 eV. This shows that Cu and Cu atoms in different orientations cause greater electronic interactions inside the GQD structure, resulting in mid-gap states that allow charge transfer. The observed band gap reduction and delocalized charge distribution significantly benefit light harvesting applications, as they allow for more efficient absorption in the visible to infrared spectrum, critical for solar energy devices. Additional modifications to the structure result in an even smaller band gap of 1.587 eV, as seen in Fig. 4. This narrowing is caused by increased hybridization between the Cu, Cu, and carbon atoms, which introduces new states near to the Fermi level and significantly alters the electronic structure. A similar pattern can be found in Fig. 3(d), where the Cu_2-4 structure exhibits comparable ecteronic disturbances and a band gap of 1.585eV. Cu_2-2 composition are suitable for optoelectronic applications because they have lower band gap, indicating improved charge transport properties.

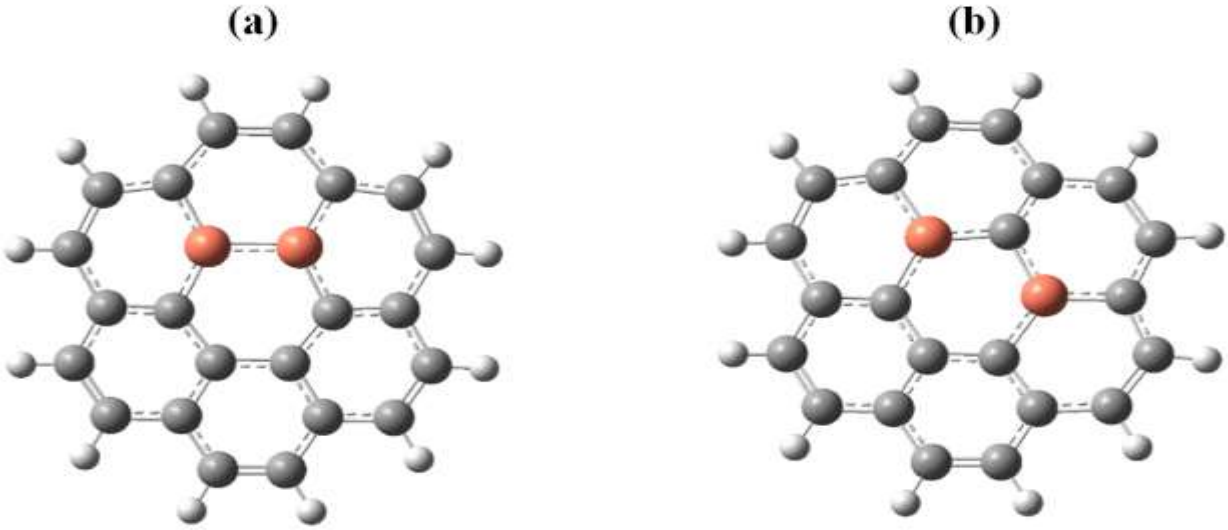

ISSN No. 2454-6194 | DOI: 10.51584/IJRIAS |Volume X Issue XII December 2025

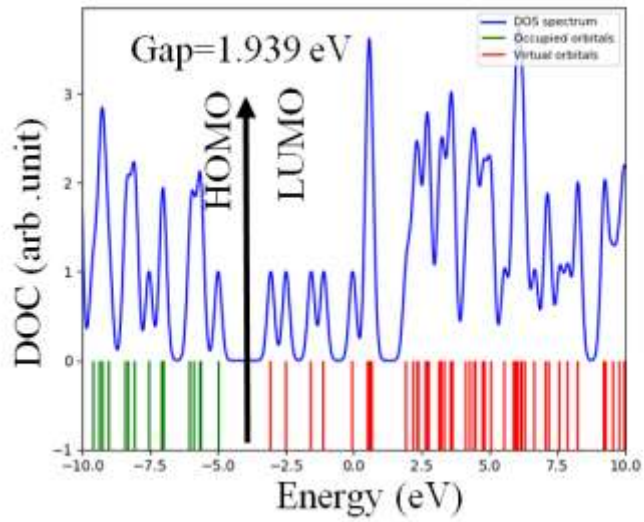

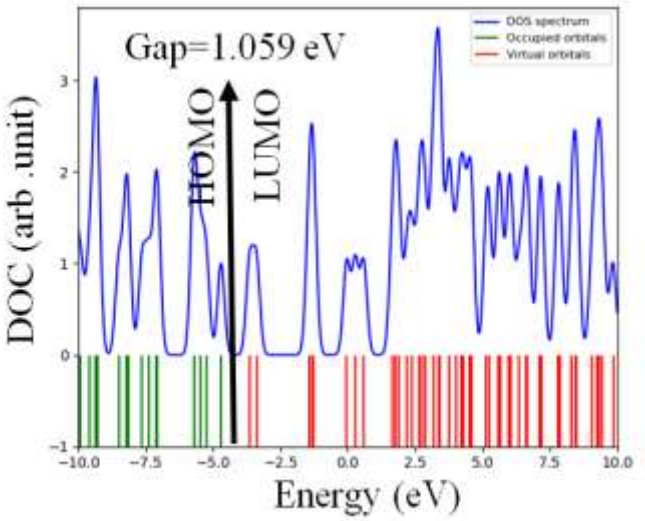

(c)

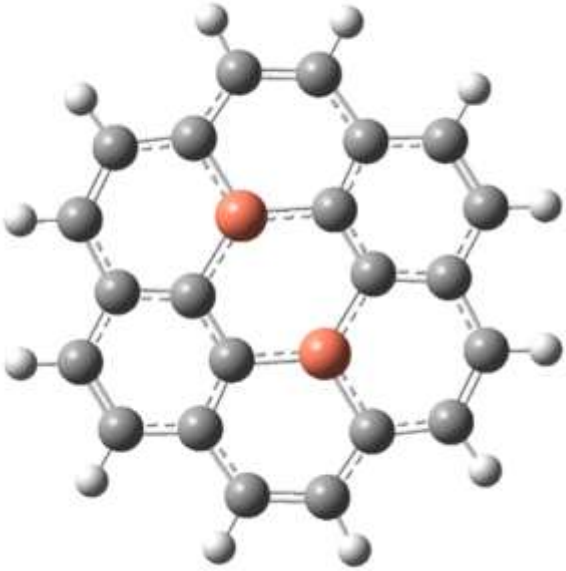

(d)

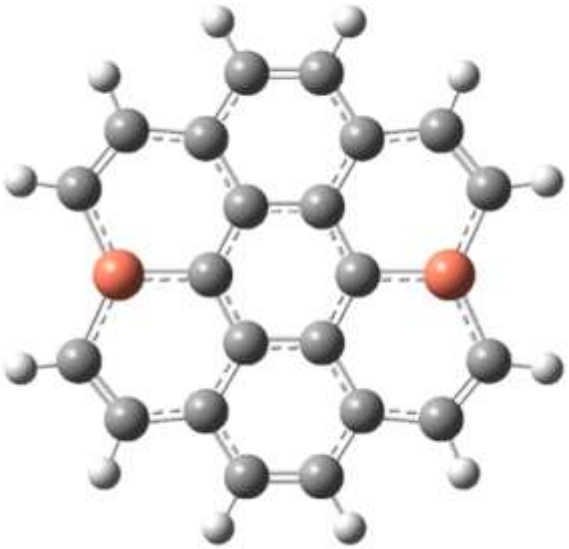

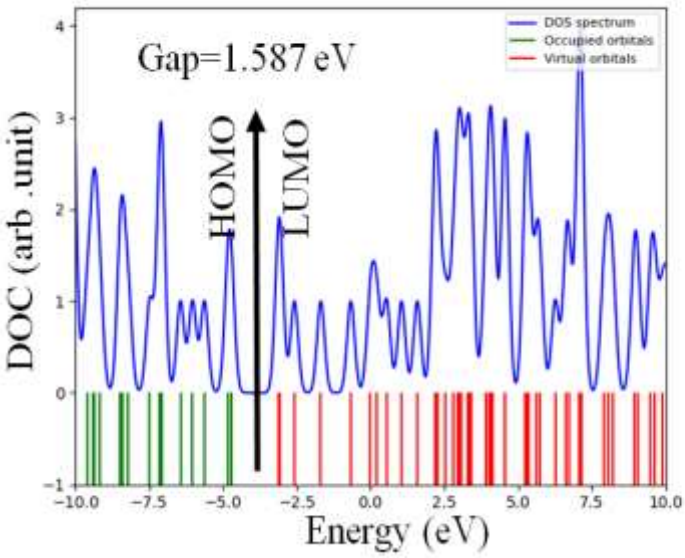

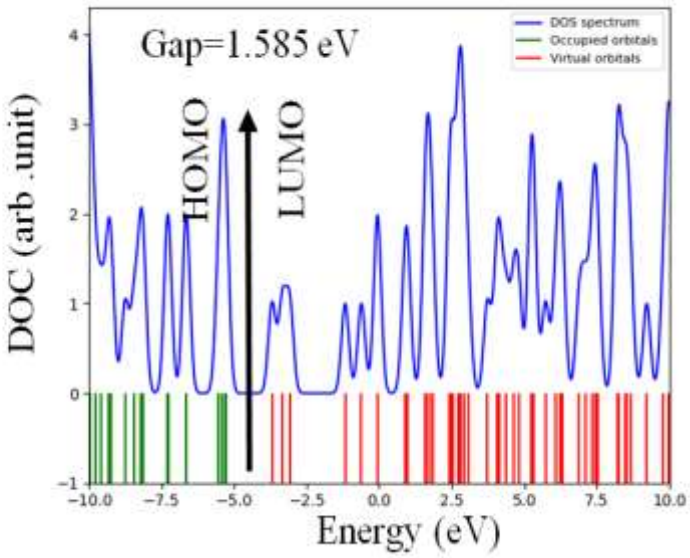

Figure 3: The structure of graphene quantum dots containing Cu dimers (**a**) Cu_2-1, (**b**) Cu_2-2, (**c**) Cu_2-3, and (**d**) Cu_2-4, together with their density of state.

ISSN No. 2454-6194 | DOI: 10.51584/IJRIAS |Volume X Issue XII December 2025

The DOS spectra reveal more details on these changes. The presence of novel electronic states induced by Cu dimers is supported by a significant redistribution of states in the occupied (green) and virtual (red) orbitals, particularly around the Fermi level. The intense contact between Cu and Cu alters the system's electronic transport behavior, resulting in a shift in state density. The expansion of DOS peaks in the Cu_2-2 arrangement suggests greater charge carrier delocalization, which improves electronic performance. The location and interaction of the Cu dimer at the second site considerably affects the band gap modulation of quantum dots. The Cu_2 functionalization allows for precise tweaking of electronic characteristics, making GQDs suitable for sophisticated nanoelectronics and optoelectronic applications.

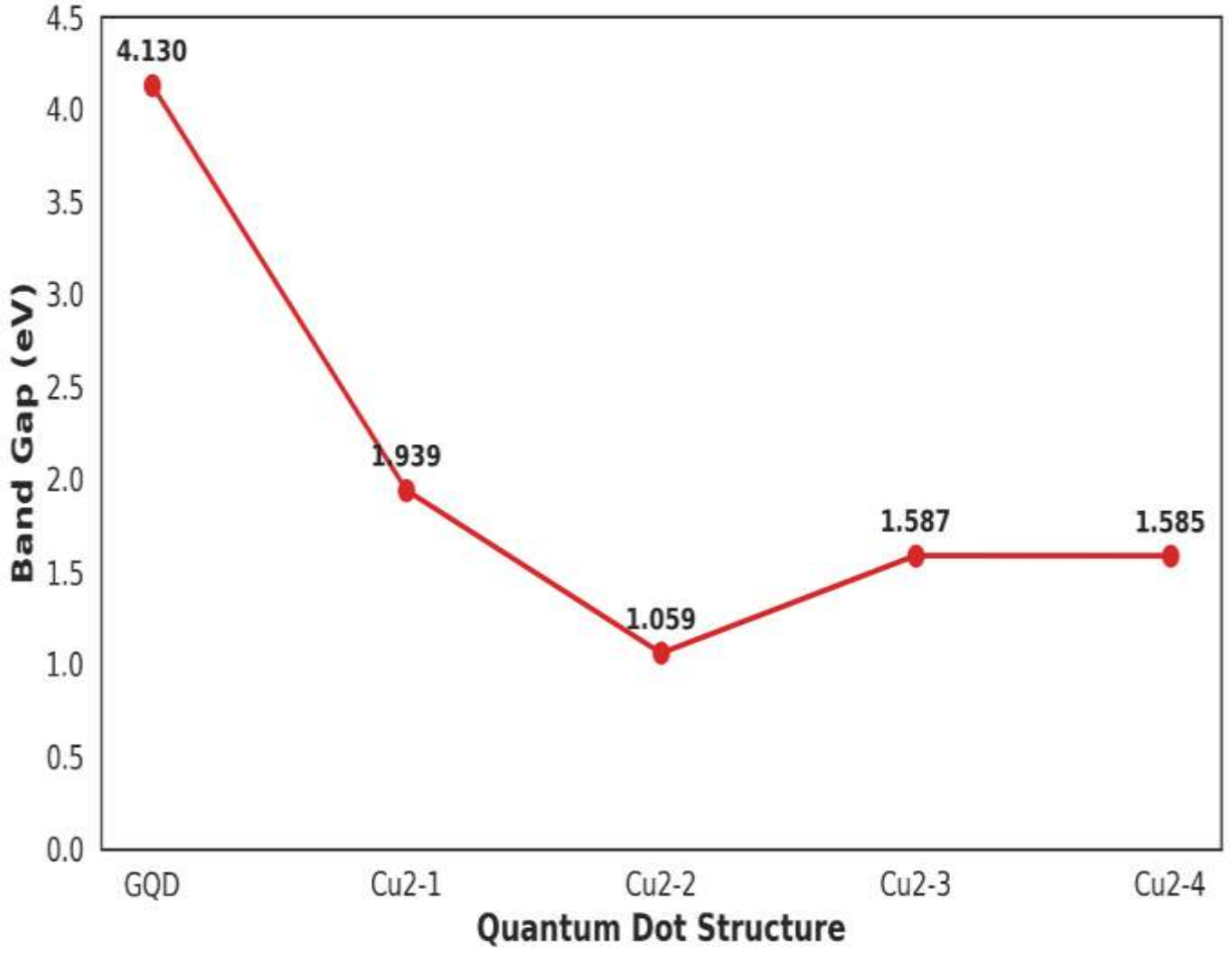

Figure 4: Band gap variation in pristine and Cu_2-doped graphene quantum dots (GQDs).

Table 1 summarizes the electronic properties of Cu-dimer-doped graphene quantum dots and pristine quantum dots. These findings shed light on how the introduction of Cu dimers affects GQDs' electronic structure and stability. The HOMO value drops from -5.413 eV in pure GQD to -4.702 eV in Cu_2-2, indicating a significant reduction in ionization potential, which enhances electron donation capability. Additionally, the LUMO energy (Cu_2-2) shifts from -1.283 eV to -3.643 eV, showing an increase in electronic affinity. As a result, the material's charge transport properties shift as the Fermi level approaches the conduction band. The most noticeable change is in the E_g, which has dropped from 4.130 eV (GQD pure) to 1.059 eV (Cu_2-2), showing a 74.359% reduction in the energy gap. The observed considerable decrease indicates that Cu dimer doping successfully boosts GQD conductivity, making them more suitable for use in optoelectronic applications. It is noted that Cu_2 doping reduces the formation energy from −256.134 eV in pure GQD to −299.282 eV, suggesting a more thermodynamically stable structure. This shows that Cu_2 insertion promotes overall stability despite potential alterations in local bonding.

ISSN No. 2454-6194 | DOI: 10.51584/IJRIAS |Volume X Issue XII December 2025

Table 1: The energetic data includes HOMO energies (E_{HOMO}), Fermi level energy (E_{FL}), LUMO energies (E_{LUMO}), energy gap (E_g), variation in E_g, (ΔE_g) , formation energies (E_F), and dipole moment (D_m in Debye) for graphene quantum dots with and without Cu dimer. All energies are in eV units.

System	E_{HOMO}	E_{FL}	E_{LUMO}	E_g	ΔE_g%	E_F	D_m
GQD pristine	-5.413	3.348	-1.283	4.130	-	-256.1	0.000012
Cu_2-1 codoped GQDs	-4.991	4.021	-3.051	1.939	-53.033	-231.8	0.423516
Cu_2-2 codoped GQDs	-4.702	4.173	-3.643	1.059	-74.359	-299.2	0.255598
Cu_2-3 codoped GQDs	-4.710	3.917	-3.123	1.587	-61.565	-230.5	0.000012
Cu_2-4 codoped GQDs	-5.277	4.485	-3.692	1.585	-61.624	-233.1	0.000036

Understanding the charge distribution and polarization features of quantum dots modified with Cu dimer requires taking the dipole moment into account. Table 1 reveals that the pristine GQD has a highly symmetric charge distribution and a very low dipole moment of 0.000012 Debye. However, the inclusion of Cu dimer dramatically alters this symmetry, resulting in significant fluctuations in dipole moment values. The Cu_2 doping induces asymmetric charge distribution due to the presence of copper atoms, resulting in localized variations in charge density. The Cu_2-2 has the highest dipole moment (0.255598 Debye), indicating the greatest charge separation in the arrangement. The increase in dipole moment is caused by the arrangement of the Cu and Cu atoms at opposite sites, which amplifies the polarization effect inside the GQD framework. The dipole moment is critical for device performance in optoelectronics and sensing technologies, so that Cu_2-doped GQDs are attractive for photovoltaic applications due to their higher dipole moments, which improve interactions with external electric fields [37, 38].

Figure 5 illustrates the optimized geometries and bond lengths of graphene quantum dots doped with Cu_2 dimers in four distinct configurations. Each arrangement introduces unique structural distortions that significantly alter the material's electronic response, as shown by DFT simulations. The Cu–Cu dimers exhibit varied spatial orientations and bonding interactions with the GQD surface, leading to changes in local symmetry and charge distribution. The Cu_2-3 configuration, in particular, displays an asymmetric dimer alignment that causes substantial bond length deviations in neighboring carbon atoms. This results in localized electronic states near the Fermi level and an increased dipole moment, which may enhance the material's responsiveness in energy-harvesting or sensing environments. In some configurations, the Cu atoms are positioned across the GQD plane, inducing bond elongation and lattice deformation that alter Cu–C and C–C interactions. Such structural variations promote charge separation and redistribution, which are key factors in improving photocatalytic activity and charge transport in energy devices. Overall, the structural tuning enabled by Cu_2 dimers offers a strategic pathway for engineering GQD-based materials tailored for energy conversion, environmental sensing, and sustainable nanoelectronics applications.

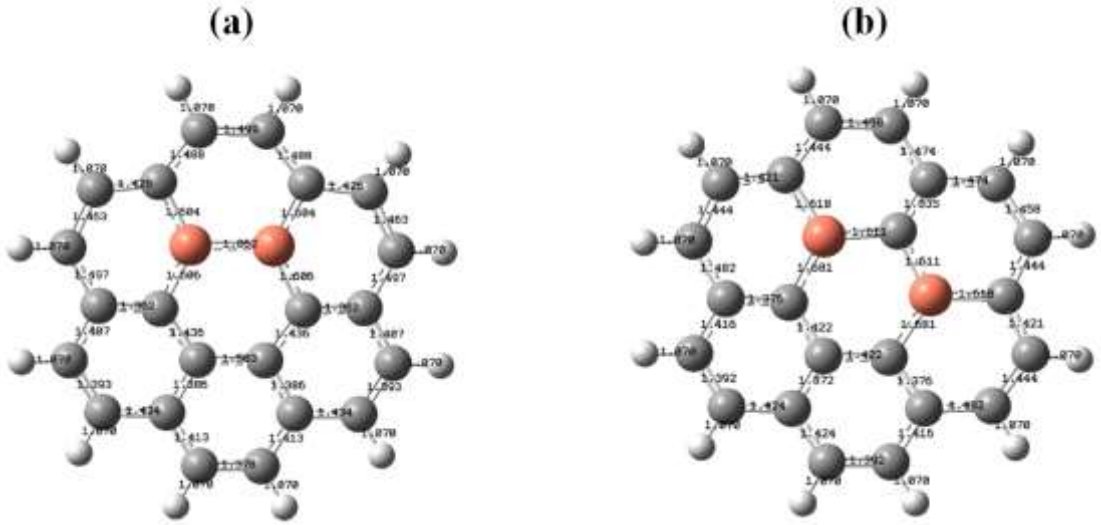

ISSN No. 2454-6194 | DOI: 10.51584/IJRIAS |Volume X Issue XII December 2025

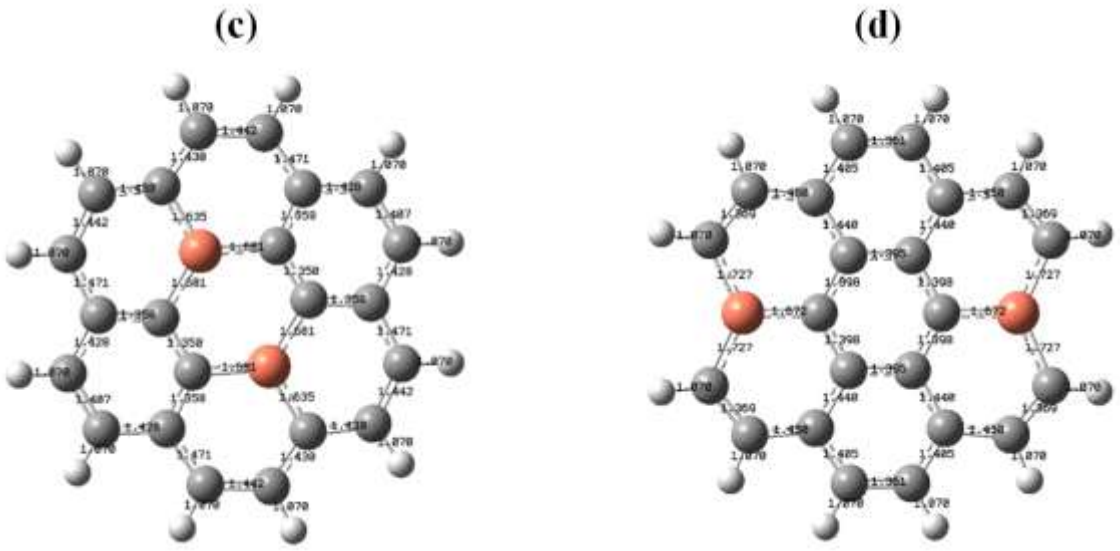

Figure 5: The organized geometries and bond lengths in the angstrom unit of the graphene quantum dot with Cu dimers produce (**a**) Cu_2-1, (**b**) Cu_2-2, (**c**) Cu_2-3, and (**d**) Cu_2-4 structures.

Figure 6 presents the molecular electrostatic potential maps of Cu_2-doped quantum dots, highlighting the charge distribution and electrostatic behavior across four configurations. The color gradients from red (low potential) to blue (high potential) visualize electron-rich and electron-deficient regions, which directly influence electronic reactivity and functional performance in energy and environmental systems. In Cu_2-1, the MEP shows a concentrated negative potential around the Cu atoms, indicating strong electron-withdrawing behavior and substantial charge transfer to the GQD surface. This redistribution suggests high reactivity, making the structure suitable for catalytic and sensing applications in environmental monitoring. The Cu_2-2 configuration exhibits a more delocalized and diffuse charge pattern, reflecting moderate electron transfer and balanced electrostatic interactions. This arrangement implies tunable reactivity and structural stability, making it a promising candidate for low-power sensing platforms and optoelectronic components in sustainable technologies.

In Cu_2-3, the potential is symmetrically distributed around the Cu sites, suggesting enhanced charge delocalization and reduced polarization. Such electrostatic uniformity indicates increased stability with localized active sites, supporting applications like selective catalysis or molecular detection in clean energy systems. The Cu_2-4 map reveals multiple localized red zones across the GQD surface, pointing to high polarization and targeted charge accumulation. This configuration may facilitate multi-site catalytic activity or high-sensitivity detection, both critical for energy harvesting and environmental remediation. The MEP analyses underscore how Cu_2 doping modulates electrostatic behavior and surface reactivity in GQDs key factors in designing advanced materials for sustainable energy conversion, pollutant sensing, and green catalytic technologies.

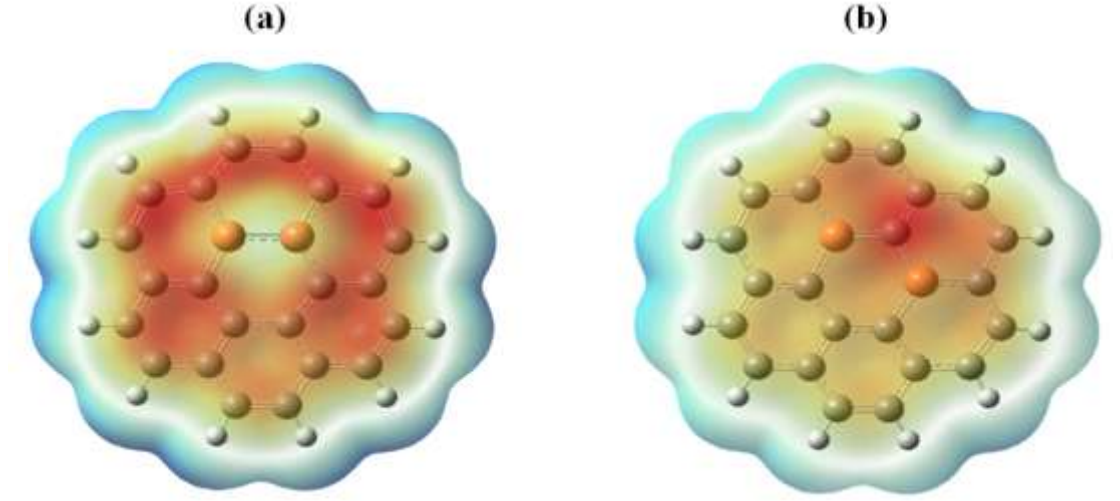

ISSN No. 2454-6194 | DOI: 10.51584/IJRIAS |Volume X Issue XII December 2025

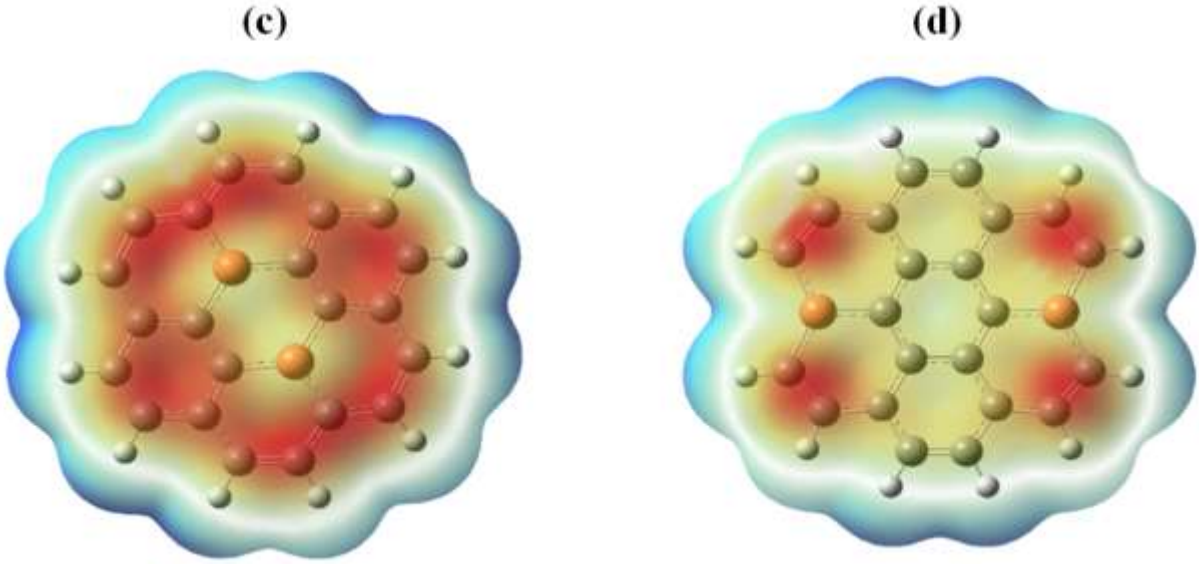

Figure 6: The molecular electrostatic potential graphic calculated in the gas phase of graphene quantum dot with Cu dimer, resulting in Cu_2-1, Cu_2-2, Cu_2-3, and Cu_2-4 structures. A spectrum of colors, with red having the lowest electrostatic potential energy values and blue having the highest.

Table 2 summarizes key chemical descriptors ionization potential, electron affinity, chemical potential, hardness, softness, and electrophilicity index that collectively reveal the electronic reactivity and environmental responsiveness of Cu_2-doped GQD systems. Doping with Cu_2 dimers reduces the ionization potential from 5.413 eV in pristine GQDs to 4.702 eV in Cu_2-2, indicating enhanced electron-donating ability. Simultaneously, the electron affinity rises, with Cu_2-2 reaching 3.643 eV, suggesting improved capacity to accept charge carriers an essential feature for energy conversion devices such as solar cells and photocatalysts. The chemical potential remains relatively stable across configurations, implying that doping does not drastically alter the average frontier orbital energy.

Table 2: The global chemical indexes: ionization potential (P), electron affinity (EA), chemical potential (μ), chemical hardness (η), chemical softness (S), and electrophilicity (ω) were determined for graphene quantum dots with and without Cu dimer. All parameters are measured in eV units.

System	*IP*	*EA*	μ	η	*S*	ω
GQD pristine	5.413	1.283	-3.348	2.065	0.484	2.714
Cu_2-1 codoped GQDs	4.991	3.051	-4.021	0.969	1.030	8.337
Cu_2-2 codoped GQDs	4.702	3.643	-4.173	0.529	1.888	16.443
Cu_2-3 codoped GQDs	4.710	3.123	-3.917	0.793	1.259	9.665
Cu_2-4 codoped GQDs	5.277	3.692	-4.485	0.792	1.261	12.691

However, the significant reduction in chemical hardness (from 2.065 eV to 0.529 eV) indicates increased susceptibility to external fields, while the corresponding rise in softness supports greater adaptability in electronic and environmental sensing applications. The electrophilicity index is a key descriptor of a material's ability to accept electrons, directly influencing its chemical reactivity and interaction with surrounding species. As illustrated in Fig. 7, the pristine GQD exhibits a low electrophilicity index (2.714 eV), indicating limited electron-accepting capability. Upon Cu_2 doping, a significant increase is observed, reaching a peak value of 16.443 eV for the Cu2-2 configuration. This dramatic enhancement suggests a greater tendency toward electron transfer, which is essential for catalytic efficiency, charge transport, and surface activity. Notably, the moderate to high ω values in Cu2-1, Cu2-3, and Cu2-4 also indicate enhanced reactivity profiles. These findings confirm that Cu_2-functionalized GQDs offer tunable electrophilic behavior, making them highly

ISSN No. 2454-6194 | DOI: 10.51584/IJRIAS |Volume X Issue XII December 2025

promising for environmentally relevant applications such as pollutant degradation, gas sensing, and energy conversion systems including fuel cells and photoelectrochemical devices.

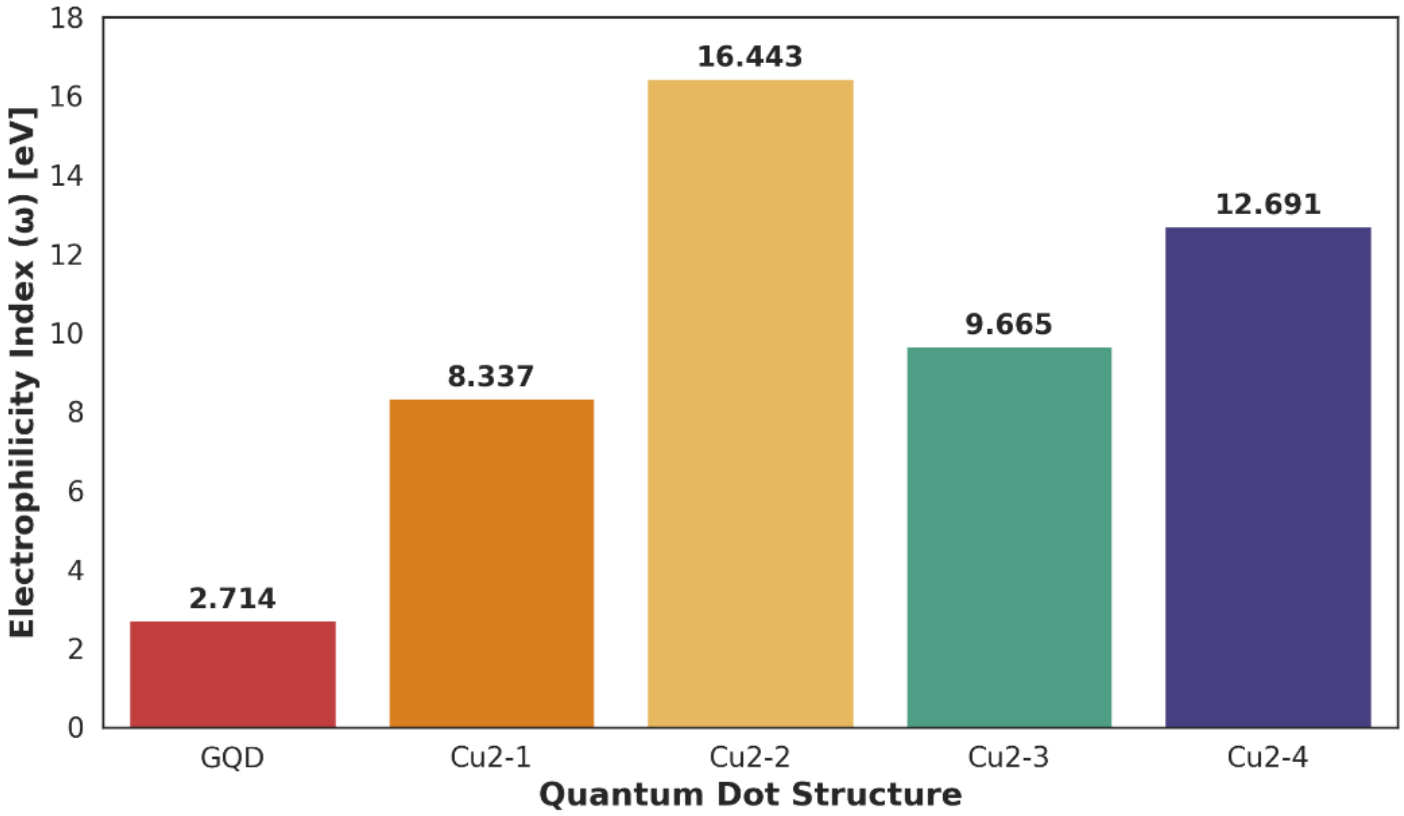

Figure 7: The electrophilicity index (ω) for pristine GQD and Cu_2-doped configurations.

Enhancing electrical conductivity (σ) is a fundamental requirement for the development of high-performance electronic and energy materials. Improved conductivity enables efficient charge transport, which is essential for the operation of devices such as solar cells, supercapacitors, and environmental sensors. In the context of Cu_2-doped GQDs, significant changes in conductivity are observed as a result of structural and electronic modifications induced by doping. As shown in Table 3, pristine GQD exhibits extremely low conductivity (1.89×10^{-31} S/m), indicating poor electron mobility and limited potential for active energy applications. However, Cu_2 doping markedly enhances the conductivity, reaching up to 1.27×10^{-5} S/m in the Cu_2-2 configuration. This increase correlates strongly with the observed band gap reduction, confirming that Cu_2 incorporation improves charge transport across the GQD matrix. The variations in conductivity across the different Cu_2 configurations further highlight the impact of Cu–Cu spatial orientation on charge dynamics. Specifically, the superior performance of Cu_2-2 underscores its suitability for next-generation optoelectronic, nanoelectronics, and energy-harvesting systems, where controlled conductivity and tunable electronic properties are crucial for sustainable operation.

Table 3. The conductivity (σ), optical absorption threshold (λ_{abs}), and corresponding absorption regions for graphene quantum dot with and without Cu dimers.

Systems	σ (S/m)	λ_{abs} (nm)	Region
GQD pristine	1.89×10^{-31}	300.2	Ultraviolet (UV) region
Cu_2-1 codoped GQDs	5.10×10^{-13}	639.2	Visible (Red) region
Cu_2-2 codoped GQDs	1.27×10^{-5}	1170.8	Infrared (IR) region
Cu_2-3 codoped GQDs	4.86×10^{-10}	781.0	Near-Infrared (NIR) region
Cu_2-4 codoped GQDs	5.08×10^{-10}	782.3	Near-Infrared (NIR) region

Tuning the optical absorption of graphene quantum dots is critical for advancing their utility in energy and environmental technologies. The pristine GQD displays an absorption onset at 300.2 nm, within the ultraviolet (UV) region suitable for high-energy applications such as UV photodetectors and sterilization systems. However, Cu_2 doping induces a pronounced redshift, extending the absorption threshold across the visible, near-infrared (NIR), and infrared (IR) regions. This shift is particularly significant in the Cu_2-2 configuration, which exhibits an absorption edge at 1170.8 nm, positioning it within the IR range ideal for thermal imaging, infrared sensing, and optical communication technologies. Cu_2-1 absorbs at 639.2 nm (visible red), enabling applications in visible-light photodetectors and bioimaging, while Cu_2-3 and Cu_2-4 show thresholds near 780 nm (NIR), suitable for non-invasive diagnostics, environmental monitoring, and fiber-optic systems. The redshift arises from the introduction of mid-gap states by the Cu dimers, which lower the optical transition energy and enhance light absorption at longer wavelengths. This broad tunability makes Cu_2-doped GQDs promising candidates for multispectral optoelectronic devices, solar energy harvesting, and environmental sensing platforms.

CONCLUSION

This study demonstrates, through density functional theory, that Cu dimer doping is a highly effective strategy for engineering the electronic and optical properties of graphene quantum dots. Cu_2 incorporation induces a substantial reduction in band gap up to 74% alongside significant improvements in electrical conductivity and charge mobility. These modifications are directly linked to enhanced energy responsiveness, which is essential for the performance of low-power and high-efficiency devices. The observed charge redistribution, increased electrophilicity, and broadened spectral absorption from UV to infrared highlight the multifunctionality of Cu_2-doped GQDs. Such characteristics make them excellent candidates for use in solar energy conversion, photodetectors, environmental sensors, and next-generation optoelectronic platforms. The engineered Cu_2-doped GQDs are promising materials for next-generation wearable energy devices, including flexible photodetectors, infrared sensors, and energy-harvesting components in wearable electronics.

Declaration of competing interest

The authors declare that they have no competing interests.

REFERENCES

1. N. Farooq et al., "Nanomaterial-based energy conversion and energy storage devices: a comprehensive review," New Journal of Chemistry, vol. 48, no. 19, pp. 8933-8962, 2024.
2. S. Tripathi et al., "Recent advances and perspectives of nanomaterials in agricultural management and associated environmental risk: a review," Nanomaterials, vol. 13, no. 10, p. 1604, 2023.
3. M. B. Kulkarni and N. Ayachit, "Energy conversion and storage devices," in Green Nanomaterials in Energy Conversion and Storage Applications: Apple Academic Press, 2024, pp. 75-93.
4. E. Roy, A. Nagar, A. Sharma, S. Roy, and S. Pal, "Graphene quantum dots and its modified application for energy storage and conversion," Journal of Energy Storage, vol. 39, p. 102606, 2021.
5. P. J. Sagayaraj et al., "Graphene quantum dots for photocatalytic CO2 reduction," Energy Technology, vol. 11, no. 11, p. 2300563, 2023.
6. T. F. Santos, D. F. Souza, E. V. Santos, B. R. Carvalho, and J. Nascimento, "Graphene and graphene quantum dots applied to batteries and supercapacitors," Nano Trends, p. 100077, 2025.
7. Q. Liu et al., "Graphene quantum dots for energy storage and conversion: from fabrication to applications," Materials Chemistry Frontiers, vol. 4, no. 2, pp. 421-436, 2020.
8. U. Masuda, S. Sahu, and L. N. Tripathi, "Recent progress and opportunities in 2D-material quantum dots: synthesis, doping, characterization, and applications," Physica Scripta, vol. 99, no. 7, p. 072002, 2024.
9. N. Zahir, P. Magri, W. Luo, J. J. Gaumet, and P. Pierrat, "Recent advances on graphene quantum dots for electrochemical energy storage devices," Energy & Environmental Materials, vol. 5, no. 1, pp. 201-214, 2022.
10. F. N. Ajeel and A. B. Ahmed, "Tuning the thermoelectric properties of graphene nanoribbons by vacancy defect with Ge-doping," Chemical Physics Impact, vol. 7, p. 100367, 2023.

11. F. N. Ajeel and A. B. Ahmed, "Influence of the boron doping and Stone–Wales defects on the thermoelectric performance of graphene nanoribbons," The European Physical Journal B, vol. 96, no. 10, p. 127, 2023.
12. P. Sharma, P. Yadav, A. Kumar, and H. Mudila, "Exploration of graphene quantum dots: Design, properties, energy storage and conversion," Journal of Power Sources, vol. 630, p. 236177, 2025.
13. L. Tang, R. Ji, X. Li, K. S. Teng, and S. P. Lau, "Energy-level structure of nitrogen-doped graphene quantum dots," Journal of materials chemistry C, vol. 1, no. 32, pp. 4908-4915, 2013.
14. S. A. Prabhu, V. Kavithayeni, R. Suganthy, and K. Geetha, "Graphene quantum dots synthesis and energy application: a review," Carbon Letters, vol. 31, no. 1, pp. 1-12, 2021.
15. G. Arora, N. S. Sabran, B. Zhang, and H. Jun, "Enhanced energy storage in electric double-layer capacitors using boron-doped graphene and upcycled carbon quantum dots derived from spent coffee grounds as electrode materials," Chemical Physics Impact, vol. 10, p. 100838, 2025.
16. S. A. Ansari, "Graphene quantum dots: novel properties and their applications for energy storage devices," Nanomaterials, vol. 12, no. 21, p. 3814, 2022.
17. P. Cui and Y. Xue, "Sulfication-induced non-radiative electron-hole recombination dynamics in graphene quantum dots for tuning photocatalytic performance," Spectrochimica Acta Part A: Molecular and Biomolecular Spectroscopy, vol. 287, p. 122117, 2023.
18. X. Niu, Y. Li, H. Shu, and J. Wang, "Revealing the underlying absorption and emission mechanism of nitrogen doped graphene quantum dots," Nanoscale, vol. 8, no. 46, pp. 19376-19382, 2016.
19. Y. A. Kumar et al., "Recent advancement in quantum dot-based materials for energy storage applications: a review," Dalton Transactions, vol. 52, no. 25, pp. 8580-8600, 2023.
20. W. Liu et al., "Graphene quantum dots-based advanced electrode materials: design, synthesis and their applications in electrochemical energy storage and electrocatalysis," Advanced Energy Materials, vol. 10, no. 29, p. 2001275, 2020.
21. G. Tatrari, M. Karakoti, M. Pathak, A. Dandapat, T. Rath, and N. G. Sahoo, "Quantum dots based materials for new generation supercapacitors application: a recent overview," in Mater. Res. Forum LLC, 2021, vol. 96, p. 215.
22. S. Srivastava, V. Malik, and M. Vishnoi, "Study on effects of quantum dots in optoelectronics and hydrogen evolution: A review," Materials Today: Proceedings, vol. 45, pp. 5672-5677, 2021.
23. M. Al Murisi et al., "New insights on applications of quantum dots in fuel cell and electrochemical systems," International Journal of Hydrogen Energy, vol. 52, pp. 694-732, 2024.
24. Z. Liu et al., "Theoretical investigation of red-shifted emission of graphitic boron doping in graphene quantum dots," Diamond and Related Materials, vol. 142, p. 110815, 2024.
25. S. K. Khamees, F. N. Ajeel, K. H. Mohsin, and M. N. Mutier, "Influence of B, Si, Ge, and As impurities on the electronic properties of graphene quantum dot: A density functional theory study," Nano Trends, vol. 7, p. 100049, 2024.
26. F. N. Ajeel, M. N. Mutier, K. H. Mohsin, S. K. Khamees, A. M. Khudhair, and A. B. Ahmed, "Theoretical Study on Electronic Properties of BN Dimers Doped Graphene Quantum dots," BioNanoScience, pp. 1-9, 2024.
27. F. N. Ajeel, K. H. Mohsin, H. G. Shakier, S. K. Khamees, and M. N. Mutier, "Theoretical insights into tunable electronic properties of graphene quantum dots through ZnO doping," Chemical Physics Impact, vol. 7, p. 100305, 2023.
28. F. N. Ajeel, S. K. Khamees, K. H. Mohsin, and M. N. Mutier, "Effect of AlN dimers on the electronic properties of graphene quantum dot: DFT investigations," Chemical Physics Impact, vol. 7, p. 100364, 2023.
29. F. N. Ajeel, Y. W. Ouda, and S. A. Abdullah, "Graphene nanoflakes as a nanobiosensor for amino acid profiles of fish products: Density functional theory investigations," Drug Invention Today, vol. 12, no. 12, 2019.
30. A. M. Khudhair, K. H. Bardan, A. Almusawe, and F. N. Ajeel, "Enhancement the electronic and optical properties for the dye Disperse Orange 13 and using in the solar cell device," in IOP Conference Series: Materials Science and Engineering, 2020, vol. 928, no. 7: IOP Publishing, p. 072031.

31. D. Maity, R. Sharma, K. R. Sahoo, A. Lal, R. Arenal, and T. N. Narayanan, "Tuning the electronic structure of monolayer Mo S 2 towards metal like via vanadium doping," Physical Review Materials, vol. 8, no. 8, p. 084002, 2024.
32. F. N. Ajeel, M. H. Mohammed, and A. M. Khudhair, "Electronic, thermochemistry and vibrational properties for single-walled carbon nanotubes," Nanoscience & Nanotechnology-Asia, vol. 8, no. 2, pp. 233-239, 2018.
33. N. M. El-Sayed, H. Elhaes, A. Ibrahim, and M. A. Ibrahim, "Investigating the electronic properties of edge glycine/biopolymer/graphene quantum dots," Scientific Reports, vol. 14, no. 1, p. 21973, 2024.
34. F. N. Ajeel, M. N. Mutier, K. H. Mohsin, S. K. Khamees, A. M. Khudhair, and A. B. Ahmed, "Theoretical Study on Electronic Properties of BN Dimers Doped Graphene Quantum dots," BioNanoScience, vol. 14, no. 2, pp. 1110-1118, 2024.
35. A. Vig, E. Doan, and K. Yang, "First-Principles Investigation of Size Effects on Cohesive Energies of Transition-Metal Nanoclusters," Nanomaterials, vol. 13, no. 16, p. 2356, 2023.
36. L. Glasser and D. A. Sheppard, "Cohesive energies and enthalpies: Complexities, confusions, and corrections," Inorganic chemistry, vol. 55, no. 14, pp. 7103-7110, 2016.
37. L. Michal et al., "Long-Range Magnetic Order in Nickel Hydroxide-Functionalized Graphene Quantum Dots," The journal of physical chemistry letters, vol. 13 49, pp. 11536-11542, 2022-12-07 2022, doi: 10.1021/acs.jpclett.2c02964.
38. A. Rad and K. Ayub, "Nonlinear optical and electronic properties of Cr-, Ni-, and Ti- substituted C20 fullerenes: A quantum-chemical study," Materials Research Bulletin, vol. 97, pp. 399-404, 2018, doi: 10.1016/J.MATERRESBULL.2017.09.036.